Bioorganic & Medicinal Chemistry 20 (2012) 3000–3008

Contents lists available at SciVerse ScienceDirect

Bioorganic & Medicinal Chemistry

journal homepage: www.elsevier.com/locate/bmc

Synthesis, biological evaluation, and molecular docking studies of benzyl, alkyl and glycosyl [2-(arylamino)-4,4-dimethyl-6-oxo-cyclohex-1-ene]carbodithioates, as potential immunomodulatory and immunosuppressive agents

El Sayed H. El Ashry [a,b,*], Mohammad R. Amer [a], Omer M. Abdalla [c], Aly A. Aly [d], Samreen Soomro [c], Almas Jabeen [c], Sobia Ahsan Halim [c], M. Ahmed Mesaik [c], Zaheer Ul-Haq [c]

[a] H.E.J. Research Institute of Chemistry, International Center for Chemical and Biological Sciences, University of Karachi, Karachi 75270, Pakistan
[b] Chemistry Department, Faculty of Science, Alexandria University, Alexandria, Egypt
[c] Dr.Panjwani Center for Molecular Medicine and Drug Research, International Center for Chemical and Biological Sciences, University of Karachi, Karachi 75270, Pakistan
[d] Chemistry Department, Faculty of Science, Benha University, Benha, Egypt

ARTICLE INFO

Article history:
Received 6 January 2012
Revised 28 February 2012
Accepted 1 March 2012
Available online 15 March 2012

Keywords:
Carbodithioate
Dimedone
Enamine
Indazolethione
Immunomodulatory
Immunosuppressive
Docking
Glycosyl

ABSTRACT

The immunomodulating properties of functionalized [2-(arylamino)-4,4-dimethyl-6-oxo-cyclohex-1-ene] carbodithioates and 6,6-dimethyl-4-(2-(propan-2-ylidene)hydrazinyl)-6,7-dihydro-2*H*-indazole-3(5*H*)-thione compounds have been investigated. Four of them, **13**, **18, 19** and **20** inhibited PBMC proliferation induced by phytohemagglutinin (PHA) in a dose dependent manner with an IC_{50} of $\leqslant$20 μM. The Th-1 cytokine, interleukin-2 (IL-2) in PHA/PMA-stimulated peripheral blood mononuclear cells (PBMCs) is significantly inhibited by **13, 19** and **20** with an IC_{50} of 8.4 ± 0.4, 5.34 ± 0.15 and 4.9 ± 0.7 μM, respectively. They also inhibited the PMA/lipopolysaccharide-induced proinflammatory cytokines, IL-1β and TNF-α production in human monocytic leukemia cells (THP-1), by 86%, 46% and 59.2% for IL-1β and by 83.8%, 48.2% and 58.7% for TNF-α, respectively. Only **20** showed significant suppressive activity against the phagocyte oxidative burst in a dose dependent manner, with an IC_{50} of 23.8 μM. LPS-induced nitrites in mouse macrophages were found to be inhibited by compounds **6, 8, 13–15** and **19** with an IC_{50}, which range between 7.7 and 63 μM. The cytotoxicity for the active compounds was also studied on Rat Wistar Hepatocyte cell line, CC1 and the Mouse Fibroblast cell line 3T3 NIH in the presence of compounds using a standard MTT assay. Furthermore, structural–activity relationship using automated docking software revealed that active compounds **7**, **13** and **19**, adapted the same binding mode, however the most active compound **20** is found deeply inserted within the ligand binding site of IL-2, as multiple hydrophobic and hydrophilic key interactions stabilize the compound inside the binding site, thus contributing higher activity.

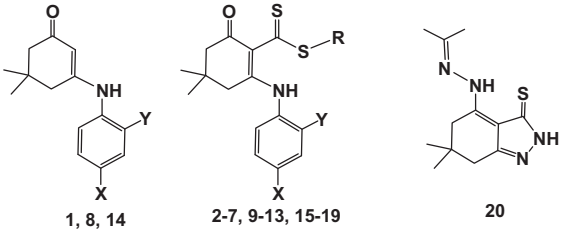

1, 8, 14 — 2-7, 9-13, 15-19 — 20

* Corresponding author.
E-mail address: eelashry60@hotmail.com (El Sayed H. El Ashry).

0968-0896/$ - see front matter © 2012 Elsevier Ltd. All rights reserved.
http://dx.doi.org/10.1016/j.bmc.2012.03.003

1. Introduction

The incorporation of dithioate functionality in a variety of compounds led to structural characteristics which, in turn influence their physical properties and their metabolic products. Thus wide spectrums of biological and industrial applications have been reported.[1–6] This class of compounds has been demonstrated to possess insecticidal, antifungal, antibacterial, antiviral and antitumor activity[7–12] as well as inhibitory action against brassinin detoxification by phytopathogenic fungus *Leptosphaeria maculans* (Phoma lingam)[13,14] potential apoptotic inducing character, and inhibition of replication of rhinovirus, influenza virus and polio virus.[10–12] Complexes of the dithioates exhibit higher antibacterial and antifungal activity than free ligand.[4] Moreover, the dithioates have modulated the function of a number of key proteins involved in apoptosis, oxidative stress, transcription, proteosome function[15] and as antioxidants as well as immunosuppressive agents.[16–18] However, few members of this class have been thoroughly investigated for immunotoxicity.[16,18,19] Thus, this class of dithioates exhibits complex biological activities including the ability to potently modulate or impair immune function.

Based on the above considerations and as reported,[20–24] we have examined the effect of a group of enamine carbodithioate and hydrazinyl-6,7-dihydro-2*H*-indazole-3(5*H*)-thione compounds **1–20** on the pro-inflammatory cytokines; IL-1β and TNFα produced by activated macrophages through toll-like receptors mediated pathogen recognition. These two cytokines are known to induce the expression of many inflammatory genes in a synergistic mode.[25] It is also reported that IL-1β in synergy with IL-2 or IL-12 in NK and T-cells induces the production of IFNγ.[26,27] We have also investigated their effect on the production of a short-lived radical, nitric oxide, produced by the enzymatic oxidation of L-arginine and the action of nitric oxide synthase.[28,29] Activated macrophages produce large amounts of nitric oxide, which is considered an essential mediator for host defence[28,29] as well as it is involved in the pathogenesis of various types of diseases.[30,31] On the other hand, we have examined the effect of enamine carbodithioates compounds on adaptive immune response through their effect on the proliferation of T cells and production of IL-2 cytokine. Th-cells secrete or stimulate the production of powerful immune factors called cytokines, which are involved in various cellular responses, such as activation, proliferation and growth. However, when overproduced they can cause serious damage, including inflammation and injury in the joints during the RA process.[32] Also abnormal Th1 immune responses have been implicated in graft rejection and other autoimmune diseases.[33,34] The effect of compounds on the production of reactive oxygen species by phagocytic cells has also been investigated. The nicotinamide adenine dinucleotide phosphate (NADPH) oxidase, located in the plasma membrane of these cells and in the membrane of specific granules, produces superoxide anion from which other reactive oxygen species (ROS) are derived. One quick and sensitive method of measuring the generation of these metabolites is chemiluminescence (CL), as described by Pavelkova & Kubala.[35] Many drugs have been developed over the last decades, including cyclosporin A (CsA), rapamycin FK506, anti-IL-2Rα antibodies (anti-Tac),[36–39] in addition to corticosteroids that up-regulates the expression of anti-inflammatory proteins, cyclophosphamides a nitrogen mustard alkylating agent, and methotrexate which acts by inhibiting the metabolism of folic acid. However, the clinical use of these immunosuppressants is hampered by side effects, and the major disadvantage being their toxicity.[40] Therefore, we studied the effects of compounds **1–20**[20,41] (Fig. 1) on different component of the immune system in order to find a lead compound as immunosuppressant.

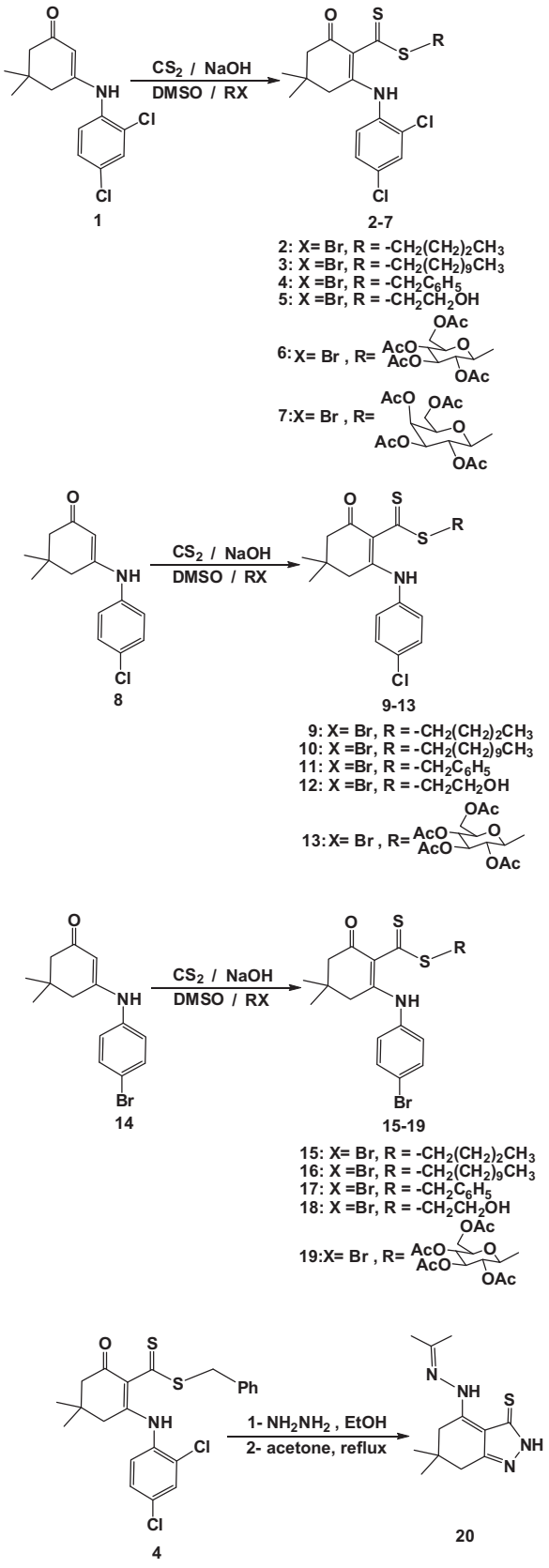

Figure 1. Structures of the investigated compounds.

Moreover, docking is frequently used to predict the binding orientation of a molecule to their protein targets which in turn

predict the affinity and activity of the small molecule. Moreover, the binding interaction of all the compounds in the ligand binding site of IL-2 was predicted by molecular docking approach.

2. Experimental section

2.1. Chemistry

Melting points were determined with a melt-temp apparatus (SMP10) in open capillaries and are uncorrected. TLC was performed on Merck silica gel 60 F_{254} with detection by UV light absorption. ^{1}H NMR spectra were recorded on Bruker Avance AV NMR spectrometer at 300 or 400 MHz, whereas the ^{13}C NMR was done on the same instrument at 75 or 100 MHz, respectively, with TMS as internal standard. Mass spectra were recorded on a Finnigan (MAT312) and Jeol (JMS.600H), HRMS were recorded with Thermo Finnegan (MAT 95XP). Solvents used were purified by simple distillation.

2.1.1. General procedure for preparation of the target compounds 1–19

A cooled solution of 3-(arylamino)-5,5-dimethyl-cyclohex-2-en-1-one (0.01 mol) and sodium hydroxide (0.4 g, 0.01 mol) in DMSO (20 mL) and water (1 mL), was treated with carbon disulfide (0.03 mol). After 20 min, alkyl halide derivatives (0.012 mol) were added and the reaction mixture was left for 24 h, then diluted with water (100 mL) and acidified with 10% hydrochloric acid. The product was purified on silica gel column chromatography (ethyl acetate:*n*-hexane 3:7) and crystallized from methanol to give a series of carboditioates.[20,41] Some of the investigated compounds have been reported in earlier publications. Thus, (2′,3′,4′,6′-tetra-*O*-acetyl-β-D-glucopyranosyl) [2-(2,4-dichlorophenylamino)-4,4-dimethyl-6-oxocyclohex-1-ene]carbodithioate (**6**),[20] (2′,3′,4′,6′-tetra-*O*-acetyl-β-D-galactopyranosyl) [2-(2,4-dichlorophenylamino)-4,4-dimethyl-6-oxocyclohex-1-ene]carbodithioate (**7**), *n*-butyl [2-(4-chlorophenylamino)-4,4-dimethyl-6-oxocyclohex-1-ene]-carbodithioate (**9**),[20] (2′,3′,4′,6′-tetra-*O*-acetyl-β-D-glucopyranosyl) [2-(4-chlorophenylamino)-4,4-dimethyl-6-oxocyclohex-1-ene]carbodithioate (**13**),[20] *n*-butyl [2-(4-bromophenylamino)-4,4-dimethyl-6-oxocyclohex-1-ene]carbodithioate (**15**),[20] (2′,3′,4′,6′-tetra-*O*-acetyl-β-D-glucopyranosyl) [2-(4-bromophenylamino)-4,4-dimethyl-6-oxocyclohex-1-ene]carbodithioate (**19**)[20] were prepared.

2.1.2. *n*-Butyl [2-(2,4-dichlorophenylamino)-4,4-dimethyl-6-oxo-cyclohex-1-ene]carbodithioate (2)

Yellow crystals, yield (34.5%), mp 128 °C, TLC (*n*-hexane/EtOAc 8:2): R_f 0.41, ^{1}H NMR ($CDCl_3$, 400 MHz) δ: 0.93 (t, 3H, J = 7.2 Hz, CH_3-4′), 1.01 (s, 6H, $2CH_3$), 1.45–1.56 (m, 2H, CH_2-3′), 1.67–1.75 (m, 2H, CH_2-2′), 2.31 (s, 2H, CH_2-3), 2.40 (s, 2H, CH_2-5), 3.14 (t, 2H, J = 7.6 Hz, SCH_2), 7.51 (d, 1H, J = 8.4 Hz, ArH), 7.31 (m, 1H, ArH), 7.51 (d, 1H, ArH), 14.73 (s, 1H, NH). ^{13}C NMR (DMSO-d_6, 125 MHz) δ: 13.5 (CH_3-4′), 21.9 (CH_2-3′), 27.3 ($2CH_3$), 28.5 (CH_2-2′), 30.9 (C-5), 35.7 (SCH_2), 41.2 (C-4), 50.8 (C-6), 118.4 (C-2), 128.1, 129.4, 130.5, 131.5, 132.5, 133.9 (ArH), 162.7 (C-1), 191.3 (C═S), 223.0 (C═O). MS-EI: *m*/*z* (%) = 415 (12), 358 (100), 326 (12), 291 (20), 186 (6), 145 (6). HRMS-EI (M^+): *m*/*z*: Calcd for $C_{19}H_{23}Cl_2NOS_2$: 415.0598, found 415.0556.

2.1.3. *n*-Undecanyl [2-(2,4-dichlorophenylamino)-4,4-dimethyl-6-oxo-cyclohex-1-ene]carbodithioate (3)

Yellow crystals, yield (31%), mp 77 °C, TLC (*n*-hexane/EtOAc 6:4): R_f 0.51, ^{1}H NMR (DMSO-d_6, 300 MHz) δ: 0.84 (t, 3H, J = 6.6 Hz, CH_3-11′), 0.95 (s, 6H, $2CH_3$), 1.23 (br s, 16H, $8CH_2$), 1.55 (m, 2H, CH_2-2′), 2.25 (s, 2H, CH_2-3), 2.37 (s, 2H, CH_2-5), 3.04 (t, 2H, J = 7.3 Hz, SCH_2), 7.37–7.47 (m, 2H, ArH), 7.74–7.78 (m, 1H, ArH), 12.12 (s, 1H, NH). ^{13}C NMR (DMSO-d_6, 125 MHz) δ: 13.8 (CH_3-11′), 21.9 (C-10′), 27.3 ($2CH_3$), 26.4, 28.4, 28.6, 28.7, 28.8, 28.9, 30.9 ($8CH_2$), 31.2 (C-5), 35.9 (SCH_2), 41.2 (C-4), 50.7 (C-6), 118.4 (C-1), 128.4, 129.4, 130.5, 131.5, 132.5, 133.9 (ArH), 162.7 (C-2), 191.2 (C═S), 222.9 (C═O). MS-EI: m/z (%) = 513 (4), 358 (100), 292 (26), 186 (5). HRMS-EI (M^+): *m*/*z*: Calcd for $C_{26}H_{37}Cl_2NOS_2$: 513.1694, found 513.1714.

2.1.4. Benzyl [2-(2,4-dichlorophenylamino)-4,4-dimethyl-6-oxo-cyclohex-1-ene]carbodithioate (4)

Red crystals, yield (31%), mp 208 °C, TLC (*n*-hexane/EtOAc 6:4): R_f 0.32, ^{1}H NMR ($CDCl_3$, 300 MHz) δ: 1.01 (s, 6H, $2CH_3$), 2.33 (s, 2H, CH_2-3), 2.40 (s, 2H, CH_2-5), 4.32 (s, 2H, SCH_2), 7.14–7.54 (m, 7H, ArH), 7.55 (s, 1H, ArH), 15.41 (s, 1H, NH). ^{13}C NMR (DMSO-d_6, 100 MHz) δ: 27.3 ($2CH_3$), 30.8 (C-5), 41.3 (C-4), 41.5 (C-6), 50.8 (SCH_2), 117.6 (C-2), 127.2, 128.4, 128.5, 129.5, 129.6, 130.4, 131.4, 133.0, 133.5, 135.3 (ArH), 165.8 (C-1), 192.1 (C═S), 219.2 (C═O). MS-EI: *m*/*z* (%) = 449 (2), 416 (2), 358 (23), 292 (24), 91 (74). HRMS-EI (M^+): *m*/*z*: Calcd for $C_{22}H_{21}Cl_2NOS_2$: 449.0442, found 449.0401.

2.1.5. 2-Hydroxyethyl [2-(2,4-dichlorophenylamino)-4,4-dimethyl-6-oxo-cyclohex-1-ene]carbodithioate (5)

Red crystals, yield (34.5%), mp 151 °C, TLC (MeOH/$CHCl_3$ 5:95): R_f 0.61, ^{1}H NMR (DMSO-d_6, 300 MHz) δ: 0.95 (s, 6H, 2 CH_3), 2.27 (s, 2H, CH_2-3), 2.36 (s, 2H, CH_2-5), 3.21 (t, 2H, J = 6.4 Hz, SCH_2), 3.62 (q, 2H, CH_2O), 4.96 (t, 1H, J = 5.2 Hz, OH), 7.41–7.51 (m, 2H, ArH), 7.80 (m, 1H, ArH), 12.21 (s, 1H, NH). ^{13}C NMR ($CDCl_3$, 125 MHz) δ: 27.9 ($2CH_3$), 30.9 (C-5), 38.8 (C-4), 42.2 (C-6), 51.7 (SCH_2), 59.5 (CH_2O), 118.5 (C-2), 128.2, 129.1, 130.4, 132.2, 133.2, 134.0 (ArH), 166.7 (C-1), 193.1 (C═S), 219.3 (C═O). MS-EI: *m*/*z* (%) = 403 (3), 359 (31), 326 (69), 282 (4), 219 (3), 185 (28). HRMS-EI (M^+): *m*/*z*: Calcd for $C_{17}H_{19}Cl_2NO_2S_2$: 403.0234, found 403.0235.

2.1.6. *n*-Undecanyl [2-(4-chlorophenylamino)-4,4-dimethyl-6-oxo-cyclohex-1-ene]carbodithioate (10)

Yellow crystals, yield (48%), mp 95 °C, TLC (*n*-hexane/EtOAc 7:3): R_f 0.79, ^{1}H NMR ($CDCl_3$, 300 MHz) δ: 0.84 (t, 3H, CH_3-11′), 0.95 (s, 6H, $2CH_3$), 1.23 (s, 16H, $8CH_2$), 1.56–1.59 (m, 2H, CH_2-2′), 2.27 (s, 2H, CH_2-3), 2.56 (s, 2H, CH_2-5), 3.06 (t, 2H, J = 7.4 Hz, SCH_2), 7.37–7.26 (d, 2H, ArH), 7.48 (d, 2H, ArH), 12.94 (s, 1H, NH). MS-EI: *m*/*z* (%) = 479 (5), 384 (6), 324 (100), 292 (73), 260 (7), 236 (9), 188 (11), 55 (75). HRMS-EI (M^+): *m*/*z*: Calcd for $C_{26}H_{38}ClNOS_2$: 479.2083, found 479.2090.

2.1.7. Benzyl [2-(4-chlorophenylamino)-4,4-dimethyl-6-oxo-cyclohex-1-ene]carbodithioate (11)

Reddish crystals, yield (49%), mp 211 °C, TLC (*n*-hexane/EtOAc 7:3): R_f 0.79, ^{1}H NMR ($CDCl_3$, 300 MHz) δ: 1.06 (s, 6H, 2 CH_3), 2.23 (s, 2H, CH_2-3), 2.63 (s, 2H, CH_2-5), 4.41 (s, 2H, SCH_2), 5.99 (s, 1H, NH), 7.19-7.26 (m, 5H, ArH), 7.38 (d, 4H, ArH). MS-FAB: *m*/*z* = 416 [M^++1]. HRMS-ESI: *m*/*z* Calcd for $C_{22}H_{23}ClNOS_2$ (M^++H) 416.0909, found 416.0920.

2.1.8. 2-Hydroxyethyl [2-(4-chlorophenylamino)-4,4-dimethyl-6-oxo-cyclohex-1-ene]carbodithioate (12)

Red crystals, yield (43%), mp 165 °C, TLC (MeOH/$CHCl_3$ 5:95): R_f 0.54, ^{1}H NMR (DMSO-d_6, 300 MHz) δ: 0.94 (s, 6H, $2CH_3$), 2.27 (s, 2H, CH_2-3), 2.56 (s, 2H, CH_2-5), 3.22 (t, 2H, J = 6.5 Hz, SCH_2), 3.63 (q, 2H, CH_2O), 4.94 (t, 1H, J = 5.3 Hz, OH), 7.20 (d, 2H, ArH), 7.61 (d, 2H, ArH), 12.83 (s, 1H, NH). MS-EI: *m*/*z* (%) = 369 (79), 336 (2), 278 (11), 130 (100).

2.1.9. *n*-Undecanyl [2-(4-bromophenylamino)-4,4-dimethyl-6-oxo-cyclohex-1-ene]carbodithioate (16)

Yellow crystals, yield (38%), mp 137 °C, TLC (*n*-hexane/EtOAc 7:3): R_f 0.70, ^{1}H NMR (DMSO-d_6, 300 MHz) δ: 0.81 (t, 3H, CH_3-11′), 0.95 (s, 6H, $2CH_3$), 1.23 (s, 16H, $8CH_2$), 1.56–1.58 (m, 2H, CH_2-2′), 2.27 (s, 2H, CH_2-3), 2.56 (s, 2H, CH_2-5), 3.04 (t, 2H, J = 7.3 Hz, SCH_2), 7.19 (d, 2H, ArH), 7.60 (d, 2H, ArH), 12.83 (s, 1H, NH). ^{13}C NMR (DMSO-d_6, 100 MHz) δ: 13.8 (CH_3-11′), 22.0 (C-10′), 26.4, 27.3, 28.5, 28.6, 28.7, 28.8, 28.9 ($7CH_2$), 30.9 (C-5), 31.2 (C-2′), 35.9 (SCH_2), 41.4 (C-4), 50.8 (C-6), 118.3 (C-2), 119.5, 127.7, 132.1, 136.4 (ArH), 163.1 (C-1), 191.4 (C=S), 221.4 (C=O). MS-EI: m/z (%) = 523 (3), 370 (67), 304 (4), 97 (20), 55 (100). HRMS-ESI: m/z Calcd for $C_{26}H_{39}BrNOS_2$ (M^++H) 524.1656, found 524.1645.

2.1.10. Benzyl [2-(4-bromophenylamino)-4,4-dimethyl-6-oxo-cyclohex-1-ene]carbodithioate (17)

Yellow crystals, yield (40%), mp 175 °C, TLC (*n*-hexane/EtOAc 7:3): R_f 0.72, ^{1}H NMR (DMSO-d_6, 300 MHz) δ: 0.92 (s, 6H, $2CH_3$), 2.30 (s, 2H, CH_2-3), 2.62 (s, 2H, CH_2-5), 4.26 (s, 2H, SCH_2), 7.26-7.38 (m, 7H, ArH), 7.65 (d, 2H, ArH), 14.18 (s, 1H, NH). MS-EI: m/z (%) = 459 (2), 370 (96), 336 (30), 245 (6), 91 (100). HRMS-EI (M^+): m/z: Calcd for $C_{22}H_{22}BrNOS_2$: 459.0326, found 459.0316.

2.1.11. 2-Hydroxyethyl [2-(4-bromophenylamino)-4,4-dimethyl-6-oxo-cyclohex-1-ene]carbodithioate (18)

Yellow crystals, Yield (43.5%), mp 136 °C, TLC (MeOH/$CHCl_3$ 5:95) R_f 0.46, ^{1}H NMR (DMSO-d_6, 300 MHz) δ: 0.94 (s, 6H, $2CH_3$), 2.27 (s, 2H, CH_2-3), 2.56 (s, 2H, CH_2-5), 3.22 (t, 2H, J = 6.4 Hz, SCH_2), 3.64 (q, 2H, CH_2O), 4.94 (t, 1H, J = 5.0 Hz, OH), 7.27 (d, 2H, ArH), 7.49 (d, 2H, ArH), 12.92 (s, 1H, NH). MS-FAB: m/z = 414 [M^++1]. HRMS-EI (M^+): m/z: Calcd for $C_{17}H_{20}BrNO_2S_2$: 413.0119, found 413.0097.

2.1.12. 6,6-Dimethyl-4-(2-(propan-2-ylidene)hydrazinyl)-6,7-dihydro-2*H*-indazole-3(5*H*)-thione (20)

Dissolve (0.3 mmol) of benzyl [2-(2,4-dichlorophenylamino)-4,4-dimethyl-6-oxocyclohex-1-ene]carbodithioate **4** in (5 mL) of methanol, and hydrazine hydrate (0.5 mL). The mixture was heated under reflux for 6 h., the product was dissolved in acetone (10 mL), and refluxed for 0.5 h., and the product was recrystallized from methanol. Yield (60%), yellow crystals, mp 262 °C; TLC (5:95 MeOH/$CHCl_3$): R_f 0.61; ^{1}H NMR (DMSO-d_6, 300 MHz): δ 1.03 (s, 6H, $2CH_3$), 2.12, 2.13 (2s, 6H, $2CH_3$), 2.46 (s, 2H, CH_2-5), 2.91 (s, 2H, CH_2-7), 12.51(s, 1H, NH), 13.99 (s, 1H, NH); ^{13}C NMR (DMSO-d_6, 125 MHz): δ 18.9, 25.1 ($2CH_3$), 27.9 ($2CH_3$), 35.7 (C-6), 37.7 (C-7), 39.0 (C-5), 107.1 (C-9), 153.2 (C=N), 162.4 (C-8), 163.2 (C-4), 164.6 (C=S); EIMS: m/z (%) = 250 (93), 209 (6), 194 (42), 178 (24), 152 (13), 138 (8), 108 (7), 82 (19), 56 (100); ESIMS: Calcd for $C_{12}H_{19}N_4S$: m/z 251.1330, found 251.1324.

2.2. Biological activities

2.2.1. T-cell proliferation assay

Fresh venous blood from a healthy donor was mixed with equal volume of incomplete RPMI-1640 media (Mediatech Inc., Herndon, VA, USA) containing 2 mM L-glutamine and 1% penicillin/streptomycin. The diluted blood was then layered onto a lymphocyte separation medium (MP Biomedicals, Inc., OH, USA) and centrifuged at 400 g for 20 min at 25 °C. The mononuclear cell layer was collected, washed with incomplete RPMI-1640 and centrifuged at 300 g for 10 min at 4 °C. The peripheral blood mononuclear cells (PBMNCs) were resuspended in RPMI-1640 complete media containing 10% fetal bovine serum from PAA laboratories GmbH Pasching, Austria. In a 96 wells round-bottomed plate (IWAKI, Scitech. DIV., Ashai Techno glass, Japan), 50 μL of cell suspension (2.5×10^6 cell/mL), 50 μL of phytohemagglutinin (PHA) for a final concentration of 5 μg/mL, 50 μL supplemented RPMI-1640 and 50 μL of test compounds in a final concentration of 0.5, 5 and 50 μg/mL (in triplicates) were added to the culture mixture. Plates were then incubated at 37 °C in a humidified atmosphere of 5% CO_2 in air for 72 h. To each well 0.5 μCi [methyl-^{3}H]-thymidine (Amersham Place Little Chalfont, Buckinghamshire, UK) was added for additional 18 h. Cells were harvested using a cell harvester (Inotech, Dottikon, Switzerland), and incorporation was measured by liquid scintillation counter (Beckman coulter, LS 6500, Fullerton, CA, USA).

2.2.2. Interleukin-2 (IL-2) assay

The PBMNCs were cultured in a 96 well flat-bottomed plate (1.0×10^5 cell/well) in the presence or absence of three concentrations of test compounds (0.5, 5, and 50 μg/mL), and phytohemagglutinin (PHA) Phorbol myristate acetate (PMA) in a final concentration of 5 ng/mL and 20 ng/mL respectively. After an incubation period of 18 h at 37 °C in a humidified atmosphere of 5% CO_2 in air, supernatant was collected for IL-2 determination. Interleukin-2 levels were measured by using enzyme-linked immunosorbent assay (ELISA) development kit (R&D systems, Minneapolis, MN, USA). In brief the procedure followed was: 96 well ELISA plates were coated with 4.0 μg/mL mouse anti-human IL-2, in PBS, pH 7.4. Then, 100 μL recombinant human IL-2 standards and culture supernatants samples were added. The plates were incubated for 2 h at room temperature and washed three times with phosphate buffered saline (PBS), followed by addition of 100 μL/well of biotinylated goat anti-human IL-2 and further incubated for 2 h at room temperature. The plates were again washed and 100 μL/well of streptavidin conjugated horse radish peroxidase was added and incubated for additional 20 min at room temperature. After three final washes, 100 μL/well of the enzyme substrate solution of H_2O_2 and tetra methyl benzidine (1:1 v/v) was added and the color allowed to develop at room temperature in the dark. Plates were then read at 450 nm in a plate reader (DIAReader GMBH, Wr. Neudorf, Austria). Results were analyzed using Microsoft Excel software.

2.2.3. TNF-α and IL-1β cytokines

Human monocytic leukemia cells (THP-1) were obtained from European Collection of Cell Cultures, UK (ECACC) and grown in RPMI-1640 supplemented with 10% FBS, 2 mmol/L L-glutamine, 5.5 mmol/L glucose, 50 μmol/L mercaptoethanol, 1 mmol/L sodium pyruvate, and 10 mmol/L HEPES (MP Biomedicals lllkirch, France), until they attained 70% confluency. Cells were then plated in 24-well tissue culture plates at a concentration of 2.5×10^5 cells/mL and were differentiated into macrophage like cells by using phorbol myristate acetate (PMA) (SERVA (Heidelberg, Germany)) at a final concentration of 20 ng/mL and incubated for 24 h at 37 °C in 5% CO_2. Cells were then stimulated with LPS (bacterial lipopolysaccharide) purchased from DIFCO Laboratories (USA) at a final concentration of 50 ng/mL and treated with compounds (25 μg/mL) and incubated for 4 h at 37 °C in 5% CO_2. The supernatant collected after 4 h incubation was analyzed for TNF-α and after 18 h incubation were analyzed for IL-1β level. Cytokines quantification in supernatants were performed by human TNF-α and IL-1β Duo set Kits (R&D systems, Minneapolis, USA) and according to manufacturers instructions.

2.2.4. Nitrite concentration in mouse macrophage culture medium

The mouse macrophage cell line J774.2 (UK ECACC) was cultured in T75 flasks in DMEM that contained 10% fetal bovine

serum supplemented with streptomycin/penicillin 1%. Flasks were kept at 37 °C in atmosphere of humidified air containing 5% CO_2. Cells (10^6 cells/mL) were then, the seeded in a 24-well plate and the nitric oxide synthase (NOS-2) in macrophages was induced by 20 μg/mL *Escherichia coli* lipopolysaccharide (DIFCO Laboratories, USA). The test compounds were added at a concentration of 25 μg/mL soon after LPS stimulation and incubated at 37 °C in 5% CO_2. Cell culture supernatant was collected after 24 h. Nitrite accumulation in J774.2 cell culture supernatant was measured using the Griess method,[42] where 50 μL of 1% sulfanilamide in 2.5% phosphoric acid, followed by 50 μL of 0.1% naphtyl-ethylene diamine dihydrochloride in 2.5% phosphoric acid were added to 50 μL of culture medium. After 10 min of incubation at 23 °C the absorbance at 550 nm was read. Micromolar concentrations of nitrite were calculated from standard curve constructed with sodium nitrite as a reference compound. Results were expressed as means ± SD of duplicate readings.

2.2.5. Chemiluminescence assay

Release of the reactive oxygen species (ROS) from whole blood phagocytes during the oxidative burst was measured by the luminol-enhanced chemiluminescence assay procedure.[35] In brief; three concentrations of each compound (1.0, 10 and 100 μg/mL) were prepared in 25 μL of Hank's balanced salt solution ($HBSS^{++}$) with calcium chloride and magnesium sulfate in half area 96 well white flat-bottomed plate (Sigma Aldrich, Germany) with a final well volume of 100 μL. Then 25 μL of whole blood diluted 1:50 in suspension of Hanks balance salt solution ($HBSS^{++}$) (Sigma, St. Louis, USA) was added. Positive and negative controls and blank wells were included. Cells and compounds were incubated for 30 min at 37 °C, then 25 μL luminol [3-aminophthalhydrazide] (Research Organics Cleveland, OH, USA), was added into each well and 25 μL serum opsonized zymosan (*Saccharomyces cerevisiae* origin) purchased from (Fluka, Buchs, Switzerland) was added except for negative and blank wells. The ROS chemiluminescence kinetic was monitored with luminometer from Labsystems Luminoskan, (Helsinki, Finland) for 50 min in the repeated scan mode. Peak and total integral chemiluminescence reading were expressed in the relative light unit.

2.2.6. Cytotoxicity assessment using MTT assay and two cell-lines

In vitro cytotoxicity assays were performed as described by Scholz et al.,[43] using the 3T3-L1 mouse embryo fibroblast cell line (American Type Culture Collection 'ATCC', Manassas, VA 20108, USA), and CC-1 cells, a Rat Wistar Hepatocyte cell line (European Collection of Cell Cultures, Salisbury, UK). The CC-1 cells were suspended in Minimum Essential Medium Eagle (MEM) supplemented with 10% FBS, 2 mM glutamine, 1% non-essential amino acids and, 20 mM HEPES. While the 3T3-L1 cells were suspended in Dulbecco's Modified Eagle's Medium (DMEM) formulated with 10% FBS. Using flat bottomed plates, both cell-lines were plated at a concentration of 6×10^4 cells/mL and incubated for 24 h at 37 °C and 5% CO_2 environment. After removal of media, cells were challenged with three different concentrations (1.0, 5.0, and 20 μg/mL) of compounds in triplicates and were then further incubated for 48 h at 37 °C in CO_2 incubator. Following exposure to each compound, cells viability was assessed by using 0.5 mg/mL of MTT (3-(4,5-dimethylthiazol-2-yl)-2,5-diphenyltetrazolium bromide) for 4 h followed by removal of supernatant and addition of DMSO to solubilize the formazan complex. Plates were read at 540 nm after one minute shaking and readings were processed using MS Excel software. Results were expressed as means ± SD of triplicate readings.

2.3. Molecular docking

All computational studies were performed on Intel® Xeon Quad Core processor runing open SUSE 10.3 OS. The crystal structure of the Interleukin-2 in complex with phenylalanine methyl ester derivative, (PDB entry code 1M48[44]) was retrieved from the RCSB Brookhaven Protein Data Bank[45] and used for docking calculations. All water molecules were removed from the original PDB crystal structure. Hydrogen atoms were added to the protein using the Biopolymer module in SYBYL 7.3 software package.[46] The structures of the ligands were constructed on ChemDraw and converted into 3D using babel 2.2. The 3D structures were imported into SYBYL 7.3 and optimized. Geometry optimizations were performed using the Tripos force field[47] with a distance-dependent dielectric and the Powell conjugate gradient algorithm. Gasteiger–Huckel charges were used for the ligands.

GOLD 3.0[48] docking suite was employed for docking studies. GOLD Score and ChemScore were chosen as a fitness function and the standard default settings were used in all calculations. Default cut off values of 2.5 Å for H bonds and 4.0 Å for Van der Waal interactions were employed. A 10.0 Å radius active site was drawn on the original position of the co-crystallized ligand and automated cavity detection was used. After docking thirty poses were saved for each ligand.

3. Results and discussion

3.1. Synthesis

The enaminones **1, 8** and **14** were prepared by reaction of dimedone with the respective aromatic amines.[21] Their reaction with electrophilic reagent as carbon disulfide in presence of sodium hydroxide was investigated, in earlier publications, to give the carbodithioate whose alkylation or glycosylation gave the respective esters.[20,41] Thus, (2′,3′,4′,6′-tetra-*O*-acetyl-β-D-glucopyranosyl) [2-(arylamino)-4,4-dimethyl-6-oxocyclohex-1-ene] carbodithioates and (2′,3′,4′,6′-tetra-*O*-acetyl-*β*-D-galactopyranosyl) [2-(arylamino)-4,4-dimethyl-6-oxocyclohex-1-ene]carbodithioates were prepared. The reaction was extended in the present work to include a variety of alkyl or glycosyl derivatives, **2–7, 9–13** and **15–19**.

The structures can be readily confirmed by studying their ^1H NMR spectra. Thus, a signal at the low field region at δ 12.12–15.41 ppm confirmed the presence of the NH group in the respective compounds. The ^{13}C NMR spectra of the carbodithioates showed signals at δ_c 191.2–193.1 ppm which confirm the presence of C=S in their structures. The X-ray analysis has confirmed the structures of some representatives.[20,41]

The hydrazone **20** was prepared by reaction of benzyl [2-(2,4-dichlorophenylamino)-4,4-dimethyl-6-oxocyclohex-1-ene]carbodithioate **4** with hydrazine hydrate followed by reaction of the product with acetone.

3.2. Biological activity

The inflammation process is a complex of cellular and biochemical events for the elimination of infectious agents. However, uncontrolled or repeated inflammation contributes to tissues damage eventually results in chronic inflammatory disorders. In the current work, we investigated in vitro the effects of series of enamine carbodithioates on the generation of ROS, reactive nitrogen species (RNS) and several cytokines in activated immune cells. Among 20 different compounds three compounds **13, 19** and **20** were found to suppress the proliferation of T-cell, and the production of IL-2, TNF-α, IL-1β and NO. This implies that these compounds may non-specifically suppress the immune system either

by forming aggregates with signaling proteins or with the activators. The potential of compound **20** could be due to the presence of an additional –NH group on 7th carbon. In addition to this we have observed that ROS was selectively inhibited by compound **20**. This inhibition could be either at the cell receptor level or due to interference with enzymes involved in the ROS generation. Moreover, these compounds also down regulated the production of TNF-α and IL-1β which are the key inflammatory cytokines produced after stimulation of monocytes/macrophage. Beside the aforementioned compounds we also found that compounds **6**, **8** and **14** effectively decreased NO production in LPS stimulated J774.2 mouse macrophage cell line. Nitric oxide (NO) mediates a variety of physiological and pathological processes including inflammatory reaction. The increased production of NO is harmful to the host, leading to chronic inflammation condition or autoimmune diseases. Therefore NO inhibition by these compounds could have therapeutic implication in inflammatory diseases. These compounds possibly work through inhibition or competition with the enzyme inducible nitric oxide synthase (iNOS), as it is known that LPS is used to trigger these pathways of NO production in macrophages.[28] We have also used the same model in our investigation. The activity of these compounds may be based on the presence of oxygen on the additional benzene ring. To validate this result, we examined the cytotoxic potential of the potent compound on two cell lines, Rat Wistar Hepatocyte cell line CC1 and Mouse Fibroblast cell line 3T3, and the tested compounds were found to be non-toxic. Moreover structure–activity relationship by docking revealed that, the most active compound **20** is located at the hydrophilic groove of IL-2 ligand binding site and is involved in multiple hydrogen bonding, hydrophobic interactions and hydrophilic interactions that stabilize the compound inside binding site. In contrast, although compound **7**, **13** and **19** are located inside the binding site, due to the lack of interaction with neighboring amino acids their activity is lower compared to compound **20**.

3.2.1. Dose–response effect on cell proliferation

To determine the immunosuppressive activity of enamine dithioate compounds, we first determined their capacity to inhibit PHA mitogen-induced cell proliferation. Compounds **13**, **18, 19** and **20** were found to have a dose dependent inhibition on the proliferation of human PBMC stimulated by PHA with an IC_{50} of

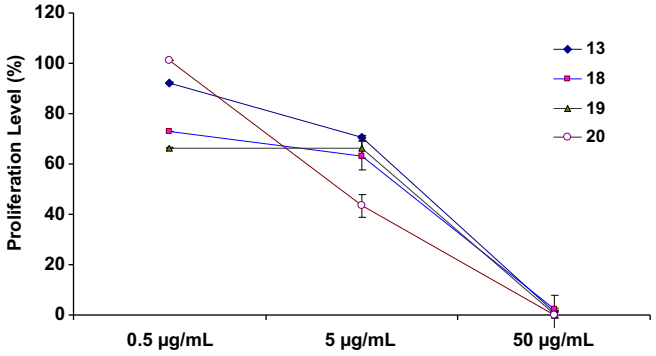

Figure 2. Dose–response curves for **13**, **18**, **19** and **20** on lymphocyte proliferation. PBMC were stimulated with PHA in the presence of increasing concentrations of the compounds. Cell proliferation was evaluated as indicated under *Materials and Methods*. Results shown are the mean ± SD of triplicate measurement expressed as percentage of stimulated control cells in the absence of compounds.

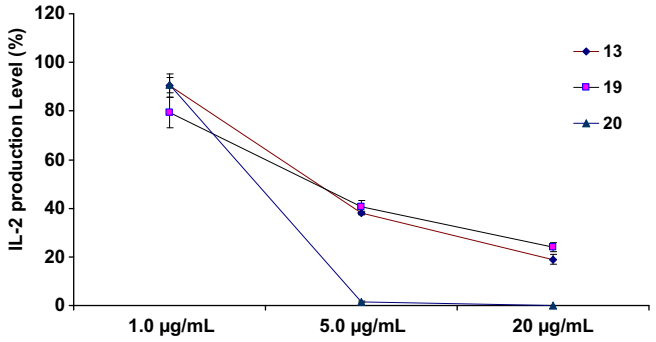

Figure 3. Dose–response curves for IL-2 production. PHA/PMA-stimulated PBMCs were incubated with three different concentrations of **13**, **19** and **20**. After 18 h the supernatant was used for the estimation of IL-2. Data are mean ± SD expressed as percentage of stimulated control cells in the absence of compounds.

Table 1
Effect of enamine dithioate compounds on T-cell proliferation, IL-2 production and on the proliferation of 3T3-L1 and CC-1 cell-lines

Compound No.	Mean ± SD of IC_{50} in µg/mL			
	T-cell proliferation	IL-2 production	Cytotoxic effect	
			3T3-L1 cell-line	CC-1 cell-line
1	17.6 ± 0.4	>20	—	—
2	>50	>20	—	—
3	>50	>20	—	—
4	>50	>20	—	—
5	>50	>20	—	—
6	15.8 ± 0.3	>20	—	—
7	3.9 ± 0.6	2.1 ± 0.1	>20	>20
8	15.0 ± 0.7	>20	—	—
9	>50	>20	—	—
10	>50	>20	—	—
11	>50	>20	—	—
12	21.0 ± 0.6	>20	—	—
13	9.9 ± 0.3	3.5 ± 0.1	>20	>20
14	>50	>20	—	—
15	>50	>20	—	—
16	>50	>20	—	—
17	>50	>20	—	—
18	8.3 ± 1.0	>20	—	—
19	8.8 ± 1.3	3.4 ± 0.5	>20	19.8 ± 0.28
20	13.2 ± 1.7	14.7 ± 1.4	—	—

Results are presented as means ± SD of triplicate measurements for IC_{50} of test compounds in each experiment. — = not determined.

Table 2
Effect of enamine dithioates (25 µg/mL) on proinflammatory cytokines (IL-1β, TNF-α) produced by macrophages

Compound No.	% Inhibition	
	IL-1β	TNF-α
1	38.5 ± 8.8	6.3 ± 5.9
2	−22.0 ± 10.7	−14.7 ± 5.9
3	30.3 ± 1.0	29.3 ± 3.0
4	−119.0 ± 5.8	−50.3 ± 8.9
5	16.5 ± 1.0	−50.3 ± 3.0
6	−273.1 ± 37.0	−48.2 ± 17.8
7	86.0 ± 1.9	83.8 ± 3.0
8	17.2 ± 5.8	−4.3 ± 3.1
9	−92.9 ± 11.7	10.5 ± 0.0
10	−15.8 ± 13.6	−56.6 ± 0.0
11	13.1 ± 0.0	−21.0 ± 3.0
12	48.1 ± 8.8	0.0 ± 14.8
13	46.8 ± 18.5	48.2 ± 5.9
14	−26.8 ± 3.9	−31.4 ± 35.6
15	−244.9 ± 10.7	−31.4 ± 17.8
16	−22.7 ± 1.9	−58.7 ± 3.0
17	−158.2 ± 4.9	−50.3 ± 8.9
18	5.5 ± 1.0	−33.5 ± 14.8
19	59.2 ± 1.0	58.7 ± 8.9

Results are expressed as means ± SD of three determinations.

15.6 ± 2.4, 15.1 ± 0.5, 20 ± 2.4 and 12.6 ± 1.4 μM, respectively (Table 1 and Fig. 2). The rest of the compounds did not show significant suppressive activity. As the IL-2 cytokine is essential for T-cell proliferation, we studied the anti-proliferative effect of **13**, **18, 19** and **20** on production of IL-2 by T-cells. These 4 compounds were found to inhibit the IL-2 production in a dose dependent manner with IC_{50} values of 8.4 ± 0.4, 5.34 ± 0.15, >48.4 and 4.86 ± 0.72 μM, respectively (Fig. 3 and Table 1). The false cytotoxic effect of these compounds was excluded by measuring the proliferation of two cell lines using standard MTT assay. No growth inhibition of the mouse embryo fibroblast cell line 3T3-L1, and a Rat Wistar Hepatocyte cell line CC-1 could be observed up to 20 μg/mL concentration tested as highest dose (Table 1).

Table 3
Effect of enamine dithioate compounds on phagocyte oxidative burst activity and nitrite production by mouse macrophages

Compound No.	IC_{50} (μg/mL) for phagocytes ROS	% of NO inhibited by 25 μg/mL test compound
1	>100	42.07
2	>100	35.17
3	>100	39.68
4	>100	39.51
5	>100	44.81
6	>100	57.18
7	5.94 ± 0.07	66.82
8	>100	62.43
9	>100	23.61
10	>100	16.48
11	>100	10.43
12	>100	43.33
13	90	77.31
14	>100	62.71
15	>100	18.92
16	>100	32.10
17	>100	38.53
18	>100	36.97
19	>100	68.41

ROS produced by human blood phagocytes and NO produced by mouse macrophages. Results are expressed as means ± SD of three determinations.

3.2.2. Effect on proinflammatory cytokines

We also observed anti-proliferative action on monocytes, and we determined the influence of the enamine thiocarbazate compounds on proinflammatory cytokines induced by LPS (Table 2). For this purpose THP-1 cells were differentiated into macrophage like cells by the action of phorbol myristate acetate (PMA) and further stimulated with LPS in the presence or absence of test compounds. The supernatants collected after 4 h incubation were analyzed for the level of TNF-α and that collected after 18 h incubation were analyzed for IL-1β level by using ELISA technique. When used in a concentration of 25 μg/mL, **13**, **19** and **20** reduced the induction of TNF-α cytokine by 83.8%, 48.2% and 58.7%, respectively and reduced the production of IL-1 β by 86%, 46.8% and 59.2% (Table 2).

3.2.3. Effect on the macrophage oxidative burst ROS and nitrites

Phagocytes play an essential role in inflammation processes. The effects of the enamine dithioate compounds on functional characteristics of human phagocytic cells have been studied and their reactive oxygen species production through a chemiluminescence assay, where certain molecules can enhance the light

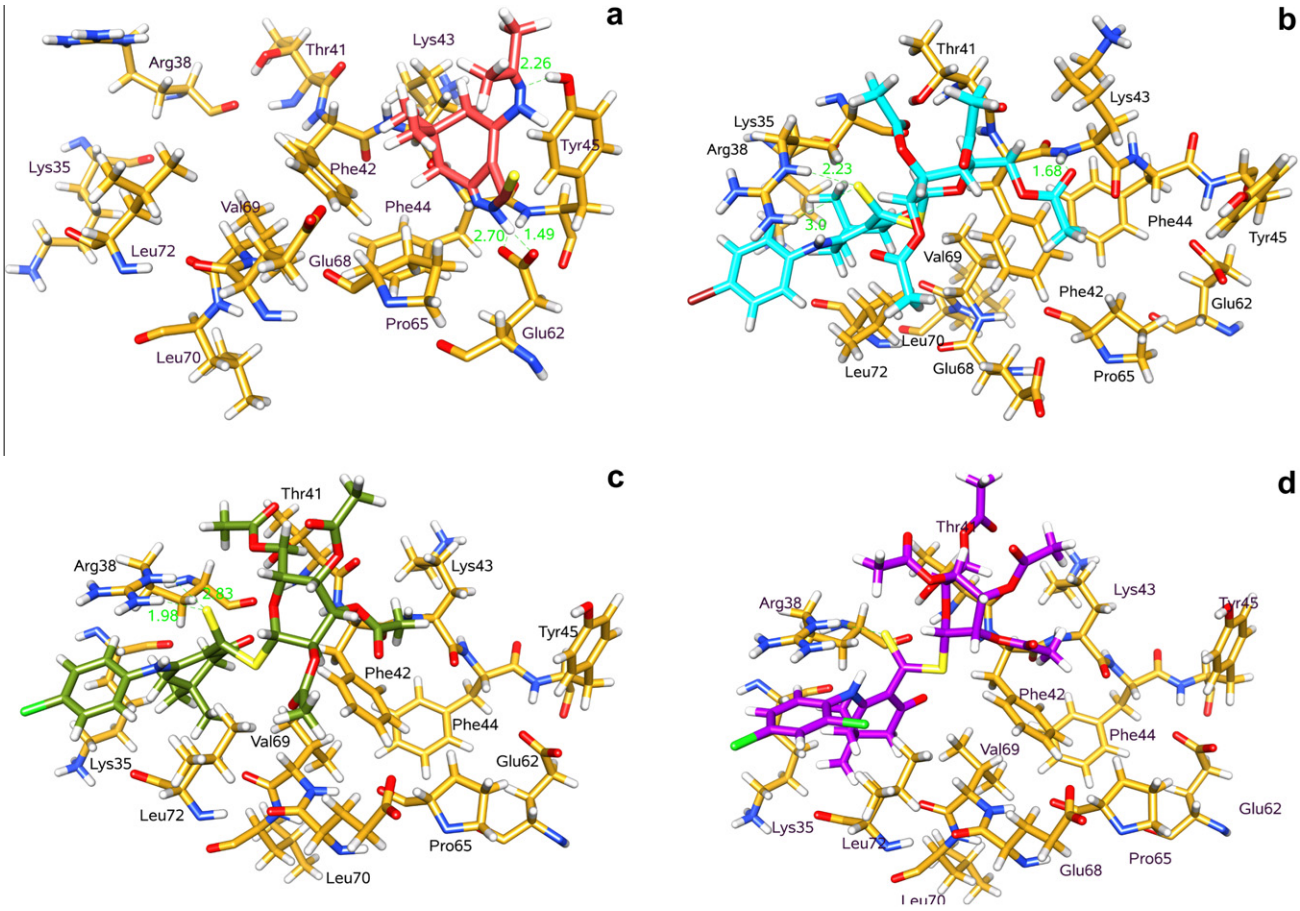

Figure 4. The docked poses of active IL-2 inhibitors: (a) 20 (pink), (b) 19 (cyan), (c) 13 (olive) and (d) 7 (purple). The interacting residues are presented in yellow stick.

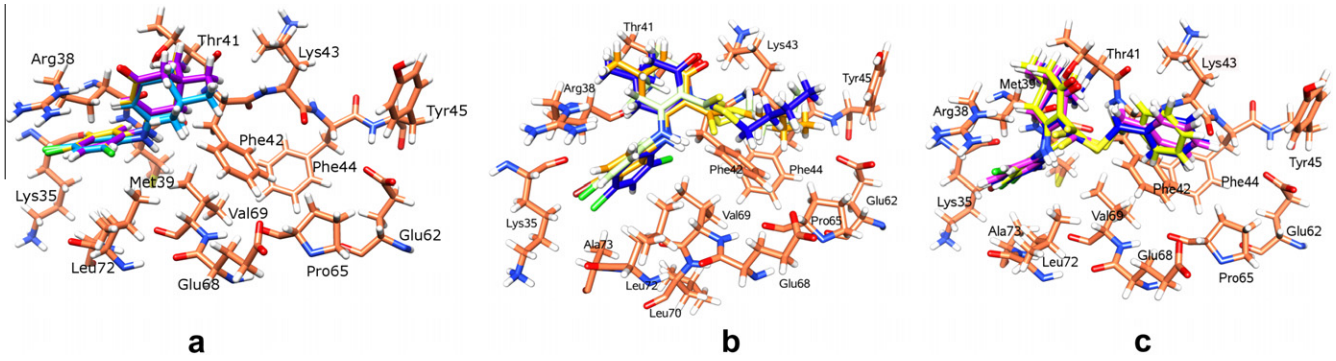

Figure 5. The binding mode of inactive compounds (a) 14 (purple), 8 (yellow), and 1 (blue) (b) 2 (blue), 15 (yellow), 9 (light-green), (c) 11 (yellow), 17 (pink) and 4 (blue). The GOLD predicted binding mode shows that all inactive compounds are surface exposed.

production to a detectable level by luminometer were determined. However, the compound **20** showed significant suppressive activity against the phagocyte oxidative burst response and ROS production in a dose dependent manner as shown in Table 3. The IC_{50} for this compound was found to be 23.8 ± 0.3 μM, while the rest of the compounds showed no activity up to a concentration of 400 μM. Moreover, effect of these compounds on nitrite accumulation by stimulated macrophages was also monitored. In this assay the LPS treated J774.2 mouse macrophage cell line has been used to study the mechanisms of nitric oxide synthase (NOS-2) induction. We studied the effect of enamine thiocarbazate compounds on nitric oxide production, out of 20 different enamines, only 6 compounds showed the nitric oxide inhibition activity with more than 50% inhibition at 25 μg/mL concentration (Table 1). Furthermore, the IC_{50} of these compounds were found to be as 49.1 ± 17.7, 16.1 ± 1.9, 63.8 ± 4.8, 7.7 ± 0.9, 44.3 ± 0.3 and 36.4 ± 1.6 μM for compounds **14, 6, 8, 19, 13** and **20**, respectively.

3.3. Molecular docking

Molecular docking is widely used in the prediction of binding mode and inhibitory mechanism of small ligands with their target protein.[49] To rationalize the structure activity relationship and to investigate the inhibitory mechanism of Enamine carbodithioate derivatives, molecular docking was efficiently realized using the automated GOLD[48] docking software. Enamine thiocarbazate derivatives were docked into the ligand binding site of IL-2[45] and their interactions and binding patterns were observed. The observed binding mode of active compounds, **6, 7, 13** and **19** and is shown in Figure 4.

The most active compound **20** is located at the hydrophilic groove of IL-2 ligand binding site and involved in multiple hydrogen bonding with the Tyr45 and Glu62, while the side chains of Phe48, Phe44 and Pro65 offers hydrophobic interaction to the compound. The NH moiety adjacent to the thiol group formed hydrogen bond with the side chain Oε1 and Oε2 of Glu62 at a distance of 2.70 and 1.49 Å, respectively. While di-methyl moiety of compound **20** is stabilized by π-CH_3 interaction provided by the side chain phenyl moieties of Phe42 and Phe44. The compound is further stabilized by the hydrophobic interaction provided by Pro65. The best docked conformation of compound **20** predicted by GOLD showed that the compound is deeply inserted within the ligand binding site of IL-2 and multiple hydrophilic and hydrophobic key interactions stabilize the compound inside the binding site, contributing to the higher activity of this compound. The observed binding mode of **20** is represented in Figure 4a.

The observed binding pattern of compound **19** reveal that the disulfide moiety is hydrogen bonded to the side chain Nε and $N\eta^2$ of Arg38. The hydrogen bond distance was 2.23 and 3.0 Å with the Nε and $N\eta^2$ of Arg38, respectively. Moreover para substituted benzene moiety is stabilized via π–cation interaction with the side chain of Arg38. The carbonyl of the acetyl moiety at the C6 of Glucose molecule is engaged in hydrogen bonding with the amide nitrogen on Lys43 at a distance of 1.68 Å. The binding pattern of **19** in the ligand binding site of IL-2 is presented in Figure 4b.

Compound **13** adopted a similar orientation to **19**. The disulfide group of the compound is hydrogen bonded to the side chain Nε and $N\eta^2$ of Arg38 with the distance of 2.83 and 1.98 Å, respectively, as observed in **19** (Fig. 4b). The acetyl moieties substituted on glucose molecule are surface exposed and not involved in interaction. The lack of interaction of these acetyl moieties with the active site amino acid residues is the reason for decreased activity of this compound. The docked orientation of **13** is shown in Figure 4c.

The docked pose of compound **7** revealed that the compound is located at the same position of **13** and **19**. The disulfide group of the compound is hydrogen bonded to the side chain Nε of Arg38 with the distance of 2.25 Å, while the hydrogen bond interaction with the $N\eta^2$ of Arg38 is lost. Similar to compound **7**, **13** and **19** also do not seem to interact with Lys43. Figure 4d reveals the binding mode of compound **7**. The binding mode analysis of compound **7** reveals that although compound is located in the ligand binding site but its acetyl substituted glucose moiety is completely surface exposed and the disulfide moiety is oriented towards the inside of

Table 4
The docking scores of enamine dithioate derivatives

Compound No.	T-cell (IC_{50}, μg/mL)	IL-2 (IC_{50}, mean ± SD)	ChemScore	GOLD score
1	17.6 ± 0.4	>20	30.29	78.66
2		>20	25.85	68.66
3		>20	22.06	53.08
4		>20	23.02	58.90
5		>20	25.30	56.30
6	15.8 ± 0.3	>20	33.63	80.01
7	3.9 ± 0.6	2.1 ± 0.1	39.51	86.81
8	15.0 ± 0.7	>20	34.09	80.56
9		>20	20.88	53.89
10		>20	22.98	53.60
11		>20	20.79	53.23
12	21.0 ± 0.6	>20	28.65	74.22
13	9.9 ± 0.3	3.5 ± 0.1	34.38	81.19
14	—	>20	27.56	52.01
15		>20	24.88	53.78
16		>20	18.90	53.60
17		>20	16.77	51.99
18	8.3 ± 1.0	>20	36.07	81.22
19	8.8 ± 1.3	3.4 ± 0.5	35.36	81.08
20		14.7 ± 1.4	32.26	68.81

Docking was performed using GOLD docking program. GOLD Score and ChemScore are summarized.

the binding cavity. Hence the absence of hydrogen bonding with Arg38 caused the loss of activity of this compound (Fig. 4d).

To explain the inactivity of compounds **1–5**, **8**–**12**, **14**–**18**, all the inactive compounds were docked in the ligand binding cavity of IL-2 by GOLD. From the docking pose, it is evident that all the inactive compounds were shown to poorly occupy the ligand binding site of IL-2. The carbonyl moiety of **1, 8** and **14** is oriented away from Arg38 and the di-methyl substituted six-member carbon ring is completely surface exposed. The docked poses are shown in Figure 5a. Similarly, the carbonyl and disulfide moieties of compounds **2, 3, 9, 10, 15** and **16** are tilted away from Arg38, while the alkyl chain at sulfide moiety is solvent exposed. The observed binding mode of compounds **2, 9** and **15** are shown in Figure 5b. The carbonyl moiety of **4, 11** and **17** is shown to be located away from Arg38 while the disulfide moiety is tilted towards the Arg38, but due to high distance, hydrogen bonding ability of the sulfone moiety is lost (Fig. 5c). Consequently, lack of interactions of those inactive compounds with key residues Arg38, Phe42, Lys43 and Phe44, might be responsible for the inactivity of these compounds in the IL-2 inhibition assay (Table 4).

4. Conclusions

The reaction of enaminones with carbon disulfide in presence of sodium hydroxide and then glycosylation gave glycosyl carbodithioates. The reaction was extended to include a variety of alkyl derivatives. A series of alkylated derivatives were tested for their effect on three immunomodulatory testing systems, T-cell proliferation, reactive oxygen and nitrogen species and cytokine studies. Our results demonstrated the potential of these compounds as anti-inflammatory agents by inhibiting the cellular immune response. Eventually, this study will help to bring about a whole new range of anti-inflammatory agents that effectively and selectively can target the mediators of the over activated immune system.

Acknowledgment

We thank the Higher Education Commission, Pakistan for the valuable support of this research project (Project No.20-697/R&D/06/38 and 20/1444/R&D/ 09/2196).

References and notes

1. Amarnath, V.; Amarnath, K.; Valentine, W. M. *Curr. Top. Toxicol.* **2007**, *4*, 39.
2. Gogoi, P. K.; Phukan, D. P.; Das, D. K. *Asian J. Chem.* **1999**, *11*, 1291.
3. Chauhan, H. P. S.; Shaik, N. M. *J. Inorg. Biochem.* **2005**, *99*, 538.
4. Eng, G.; Song, X.; Duong, Q. *Appl. Organomet. Chem.* **2003**, *17*, 218.
5. Viquez, O. M.; Lai, B.; Ahn, J. H.; Does, M. D.; Valentine, H. L.; Valentine, W. M. *Toxicol. Appl. Pharmacol.* **2009**, *239*, 71.
6. Bach, S. P.; Chinery, R.; O'Dwyer, S. T.; Potten, C. S.; Coffey, R. J.; Watson, A. J. *Gastroenterology* **2000**, *118*, 81.
7. Daniel, K. G.; Chen, D.; Orlu, S.; Cui, Q. C.; Miller, F. R.; Dou, Q. P. *Breast Cancer Res.* **2005**, *7*, 897.
8. Trevisan, A.; Marzano, C.; Cristofori, P.; Borella Venturini, M.; Giovagnini, L.; Fregona, D. *Arch. Toxicol.* **2002**, *76*, 262.
9. Huang, W.; Ding, Y.; Miao, Y.; Liu, M.-Z.; Li, Y.; Yang, G.-F. Synthesis and antitumor activity of novel dithiocarbamate substituted chromones *Eur. J. Med. Chem.* **2009**, *44*, 3687.
10. Si, X.; McManus, B. M.; Zhang, J.; Yuan, J.; Cheung, C.; Esfandiarei, M.; Suarez, A.; Morgan, A.; Luo, H. *J. Virol.* **2005**, *79*, 8014.
11. (a) Sofuoglu, M.; Kosten, T. R. *CNS Drugs* **2005**, *19*, 13; (b) Noboru, U.; Kunio, O. *J. Antimicrob. Chemother.* **2003**, *52*, 8; (c) Uchide, N.; Ohyama, K.; Bessho, T.; Yuan, B.; Yamakawa, T. *Antiviral Res.* **2002**, *56*, 207.
12. Fang, I. M.; Yang, C. H.; Lin, C. P.; Yang, C. M.; Chen, M. S. *Ocul. Pharmacol. Ther.* **2005**, *21*, 95.
13. Soledade, M.; Pedras, C.; Jha, M. *Bioorg. Med. Chem.* **2006**, *14*, 4958.
14. Güzel, O.; Salman, A. *Bioorg. Med. Chem.* **2006**, *14*, 7804.
15. (a) Yin, H. D.; Xue, S. C. *Appl. Organomet. Chem.* **2006**, *20*, 283; (b) Tabassum, S.; Pettinari, C. *J. Organomet. Chem.* **2006**, *691*, 1761; (c) Pellerito, C.; D'Agati, P.; Fiore, T.; Mansueto, C.; Mansueto, V.; Stocco, G.; Nagy, L.; Pellerito, L. *J. Inorg. Biochem.* **2005**, *99*, 1294; (d) Milacic, V.; Dou, Q. P. *Coord. Chem. Rev.* **2009**, *253*, 1649; (e) Zhang, X.; Frezza, M.; Milacic, V.; Ronconi, L.; Fan, Y.; Bi, C.; Fregona, D.; Dou, Q. P. *J. Cell. Biochem.* **2010**, *109*, 162.
16. Pyatt, D. W.; Gruntmeir, J.; Stillman, W. S.; Irons, R. D. *Toxicology* **1998**, *128*, 83.
17. Padgett, E. L.; Barnes, D. B.; Pruett, S. B. J. Toxicol. Environ. *Health* **1992**, *37*, 559.
18. Pruett, S. B.; Barnes, D. B.; Han, Y. C.; Munson, A. E. *Fundam. Appl. Toxicol* **1992**, *18*, 40.
19. Lombardi, P.; Fournier, M.; Bernier, J.; Mansour, S.; Neveu, P.; Krzystyniak, K. *Int. J. Immunopharmacol.* **1991**, *13*, 1073.
20. El Ashry, E. S. H.; Aly, A. A.; Amer, M. R.; Shah, M. R.; Ng, S. W. *Carbohydr. Res.* **2011**, *346*, 169.
21. Greenhill, J. V. *J. Chem. Soc. Perkin Trans. 1* **1976**, *20*, 2207.
22. Tominaga, Y.; Okuda, H.; Kohra, S.; Mazume, H. *J. Heterocycl. Chem.* **1991**, *28*, 1245.
23. Yoshinori, T.; Hajime, N.; Chizuko, K.; Toshiyuki, M.; Yuji, M.; Akira, H. *Heterocycles* **1990**, *31*, 1.
24. Tu, S.; Zhang, Y.; Jiang, B.; Jia, R.; Zhang, J.; Ji, S. *Synthesis* **2006**, 3874.
25. Raquel, M. R.; Yashaswini, K.; Anasuya, S.; Vedavathi, B.; Mark, D. *Cytokine* **2008**, *44*, 234.
26. Tominaga, K.; Yoshimoto, T.; Torigoe, K.; Kurimoto, M.; Matsui, K.; Hada, T.; Okamura, H.; Nakanishi, K. *Int. Immunol.* **2000**, *12*, 151.
27. Cooper, M.; Fehniger, T.; Ponnappan, A.; Mehta, V.; Wewers, M.; Caligiuri, M. *Eur. J. Immunol.* **2001**, *31*, 792.
28. Nathan, C. *FASEB J.* **1992**, *6*, 3051.
29. Nussler, A.; Billar, T. *J. Leukocyte Biol.* **1993**, *54*, 171.
30. Corbett, J.; Wang, J.; Hughes, J.; Wolf, B.; Sweetland, M.; Lancaster, J.; Mcaniel, M. *J. Biochem.* **1992**, *787*, 229.
31. Fabian, R.; Rea, H. *J. Neuroimmunol.* **1993**, *44*, 95.
32. Sadlack, B.; Merz, H.; Schorle, H.; Schimpl, A.; Feller, A. C.; Horak, I. *Cell* **1993**, *75*, 253.
33. Le Moine, A.; Goldman, M.; Abramowicz, D. *Transplantation* **2002**, *73*, 1373.
34. Singh, V. K.; Mehrotra, S.; Agarwal, S. S. *Immunol. Res.* **1999**, *20*, 147.
35. Pavelkova, M.; Kubala, L. *Luminescence* **2004**, *19*, 37.
36. Brown, E.; Schreiber, S. *Cell* **1996**, *86*, 517.
37. Wiederrecht, G.; Sabers, C.; Brunn, G.; Martin, M.; Dumont, F.; Abraham, R. *Prog. Cell Cycle Res.* **1995**, *1*, 53.
38. Schreiber, S. *Science* **1991**, *251*, 283.
39. Waldmann, T.; O'Shea, J. *Curr. Opin. Immunol.* **1998**, *10*, 507.
40. Michael, D.; David, S. *Proc. Am. Thorac. Soc.* **2005**, *2*, 449.
41. (a) El Ashry, E. S. H.; Amer, M. R.; Shah, M. R.; Ng, S. W. *Acta Cryst.* **2009**, *E65*, o2459; (b) El Ashry, E. S. H.; Amer, M. R.; Shah, M. R.; Ng, S. W. *Acta Cryst.* **2009**, *E65*, o1106; (c) El Ashry, E. S. H.; Amer, M. R.; Shah, M. R.; Ng, S. W. *Acta Cryst.* **2009**, *E65*, o597; (d) El Ashry, E. S. H.; Amer, M. R.; Shah, M. R.; Ng, S. W. *Acta Cryst.* **2009**, *E65*, o598; (e) El Ashry, E. S. H.; Amer, M. R.; Shah, M. R.; Ng, S. W. *Acta Cryst.* **2009**, *E65*, o599; (f) El Ashry, E. S. H.; Amer, M. R.; Shah, M. R.; Ng, S. W. *Acta Cryst.* **2009**, *E65*, o600; (g) El Ashry, E. S. H.; Amer, M. R.; Shah, M. R.; Ng, S. W. *Acta Cryst.* **2009**, *E65*, o601; (h) El Ashry, E. S. H.; Amer, M. R.; Shah, M. R.; Ng, S. W. *Acta Cryst.* **2009**, *E65*, o602.
42. Andrade, M. A.; Lucas, M. S.; Arellano, J. L. P.; Barreto, C. P.; Valladares, B.; Espinoza, E.; Muro, A. *Nitric Oxide* **2005**, *13*, 217.
43. Scholz, G.; Pohl, I.; Genschow, E.; Klemm, M.; Spielmann, H. *Cells Tissues Organs.* **1999**, *165*, 203.
44. Berman, H. M.; Westbrook, J.; Feng, Z.; Gilliland, G.; Bhat, T. N.; Weissig, H.; Shindyalov, I. N.; Bourne, P. E. *Nucl. Acids. Res.* **2000**, *28*, 235.
45. Michelle, R.; Arkin, M.; Randal, W. L.; DeLano, J.; Hyde, T. N.; Luong, J. D.; Oslob, D. R.; Raphael, L.; Taylor, J. W.; Robert, S. M.; James, A. W.; Andrew, C. B. *Proc. Natl. Acad. Sci. U.S.A.* **2003**, *100*, 1603.
46. SYBYL Molecular Modeling Software version 7.3, 2006.
47. Tripos Associates, St. Louis. MO.
48. GOLDv3.0. Cambridge Crystallographic Data Center, Cambridge, UK. 2006.
49. Huang, S. Y.; Zou, X. *Protein Sci.* **2007**, *16*, 43.